Catal Lett (2013) 143:829–838
DOI 10.1007/s10562-013-1040-4

Synthesis of Methyl Methacrylate by Aldol Condensation of Methyl Propionate with Formaldehyde Over Acid–Base Bifunctional Catalysts

Bin Li · Ruiyi Yan · Lei Wang · Yanyan Diao · Zengxi Li · Suojiang Zhang

Received: 22 April 2013 / Accepted: 2 June 2013 / Published online: 14 June 2013

Abstract Supported cesium catalysts with various carriers (SiO_2, Al_2O_3, TiO_2, MgO) were prepared and characterized by X-ray diffraction, BET nitrogen adsorption–desorption, NH_3 and CO_2-TPD methods and thermogravimetric analysis. Experimental results showed that the Zr–Mg–Cs/SiO_2 catalyst exhibited moderate activity for aldol condensation of methyl propionate with formaldehyde (FA) to produce methyl methacrylate. Though the activity of Zr–Mg–Cs/SiO_2 catalyst decreased with the time-on-stream, the deactivated catalyst was completely regenerated by calcination. The catalyst was regenerated 16 times and total operation time was over 500 h, its activity was identical with that of the fresh catalyst.

Keywords Aldol condensation · Catalyst · Methyl methacrylate · Methyl propionate · Formaldehyde

1 Introduction

Methyl methacrylate (MMA) and methacrylic acid (MAA) are high-value polymer intermediate, which are widely used for producing polymethyl methacrylate (so-called organic glasses) or producing polymer dispersions for paints and coating [1]. Most of MAA and MMA are produced by the traditional Acetone Cyanohydrin process (ACH). In this route, acetone and hydrogen cyanide react to product cyanohydrin, which subsequently react with sulfuric acid to form methacrylamide sulfate. The methacrylamide sulfate is either hydrolyzed to MAA and ammonium sulfate or converted to a mixture of MAA and MMA in a combined hydrolysis–esterification step with methanol. However, the ACH route needs to utilize highly toxic hydrogen cyanide and corrosive, concentrated sulfuric acid that are extremely harmful to human and environment. In recent years, the environmental pressures against shipment of HCN have forced many manufacturers to abandon utilizing HCN. Besides, disposal of spent sulphuric acid/ammonium sulphate has been another source of headaches which needs to the installation of device for thermal decomposition of the salt and recovery of sulphuric acid for recycling [2, 3]. Therefore, many researchers make a lot of efforts to develop an environmentally friendly product of MMA. Therefore, much patented work has been devoted to investigation on the aldol-condensation reaction of propionate derivatives (propionic acid and methyl propionate) with formaldehyde to produce MAA and MMA [4–6].

$$CH_3CH_2COOH + HCHO \rightarrow CH_2{=}C(CH_3)COOH + H_2O$$

$$CH_3CH_2COOCH_3 + HCHO \rightarrow CH_2{=}C(CH_3)COOCH_3 + H_2O$$

It is known that the synthesis of MAA and MMA is much more difficult than that of acrylic acid and methyl acrylate obtained by aldol condensation of acetic acid and methyl acetate, respectively, with HCHO. Both acid and base catalysts are known to be active in the reaction. About

B. Li · Z. Li (✉)
College of Chemistry and Chemical Engineering, University of Chinese Academy of Sciences, Beijing 100049, People's Republic of China
e-mail: zxli@home.ipe.ac.cn

R. Yan · L. Wang · Y. Diao · S. Zhang (✉)
Beijing Key Laboratory of Ionic Liquids Clean Process, Institute of Process Engineering, Chinese Academy of Sciences, Beijing 100190, People's Republic of China
e-mail: sjzhang@home.ipe.ac.cn

the reaction between PA and HCHO, plenty of papers and patents have been published [7–16]. On the other hand, there are limited reports on the reaction between MP and HCHO. Gogate et al. [17] reported a 10.5 % yield of MMA (based on MP) in the aldol condensation of MP with HCHO over a V–Si–P ternary catalyst. Ai [18] reported the conversion reached 14.2 % (based on MP) and 85.9 % of selectivity to MMA over a silica-supported cesium hydroxide catalyst. The mechanism for the reaction is as follows [17]:

- Activation of reactant by basic sites of the catalyst

$$R{-}CH_2{-}X + B \rightarrow R{-}{}^{-}CH{-}X + BH^{+} (B = O^{-} \text{ or } OH^{-},\ R = CH_3,\ X = COOCH_3)$$

- Activation of HCHO by acidic sites of the catalyst

$$HCHO + H^{+} \rightarrow H_2C^{+}OH$$

- Reaction of two intermediate molecules to form an aldol followed by dehydration

$$R{-}{}^{-}CH{-}X + H_2C^{+}OH \rightarrow H_2C(OH){-}C(H)R{-}X \rightarrow H_2C = CR{-}X + H_2O$$

Although the condensation route involves fewer steps than the ACH process, a major disadvantage is that the single-pass yield of MMA in the condensation reaction is relatively low, resulting in extensive recycle of the unreacted starting materials. Here our contribution is aimed to prepare more effective catalysts for the production of MMA.

2 Experimental

2.1 Catalyst Preparation

Silica and γ-alumina were obtained from commercial companies. For the Zr–Mg–Cs/SiO_2 catalyst, silica was dried first at 500 °C for 3 h and then impregnated with an aqueous solution containing desired amount of zirconium nitrate, magnesium nitrate and cesium nitrate. This mixture was oscillated at 40 °C for 24 h and then dried in an oven. The resulting solid was calcined in flowing air at 350, 400, 450, 500, 550 and 600 °C for 3 h, respectively. Cesium-impregnated alumina (Zr–Mg–Cs/Al_2O_3) was prepared in a similar method and calcined in flowing air at 450 °C. For Zr–Mg–Cs/TiO_2 catalyst, aqueous ammonia (28 %) was added dropwise with vigorously stirring into a solution of 0.2 mol/L Ti(SO_4) to obtain hydroxides until pH reached 8. The solution containing precipitation was kept in a water bath warmed at 70 °C for 5 h, and then filtered and washed with deionized water, and dried at 110 °C for 12 h. The resulting powder was impregnated with a mixed aqueous solution of zirconium nitrate, magnesium nitrate and cesium nitrate under continuous stirring at room temperature for 5 h and then dried at 110 °C for 12 h. The prepared precursor was calcined in flowing air at 450 °C. The Zr–Mg–Cs/MgO catalyst was prepared by the similar process with Zr–Mg–Cs/TiO_2 catalyst. Adding elements magnesium and zirconium, can effectively improve the performance of the catalyst. For all these catalysts, the content of zirconium and magnesium were 0.033 and 0.025 wt%, respectively [13]. The loading amounts of the catalysts were based on the quality of the carriers.

2.2 Catalyst Characterization

X-ray diffraction (XRD) patterns of catalysts were recorded by X'Pert PRO MPD diffractometer operated at an accelerating voltage of 40 kV and an emission current of 40 mA with Cu Kα radiation. The angle (2θ) was measured in steps of 0.41778°/s between 5° and 90°.

Weight loss and temperature associated with phase transformation were determined by thermogravimetry and differential thermal analysis (TG/DTA) on a Shimadzu DTG-60H analyzer. The fresh samples of catalysts before calcination were heated from room temperature to 800 °C at rate of 10 °C/min in nitrogen flow (30 mL/min).

The BET specific surface area and the pore size were obtained from nitrogen absorption and desorption isotherm method at liquid nitrogen temperature on a Quanta Chrome Instrument NOVA 2000. Prior to analysis, samples were degassed at 300 °C for 10 h.

The adsorption of CO_2 and NH_3 was measured on an Autochem II 2920 apparatus from Micromeritics. In a typical experiment, 40 mg of samples were placed in a quartz tube and was pretreated in a helium flow at 450 °C at a heating rate of 10 °C/min and the sample was kept at this temperature for 1 h. The temperature was then reduced to 50 °C prior to adsorption. 10 % NH_3–He or 10 % CO_2–He passed over the samples for 30 min at 50 °C. After purging with pure helium at 50 °C for 1 h until the baseline was stable, the desorption profile was measured by the thermal conductivity detector in helium flow at a heating rate of 10 °C/min to 500 °C.

The cesium, magnesium and zirconium in the Zr–Mg–Cs/SiO_2 were measured using inductively coupled plasma (ICP). A SHIMADZU ICPE-9000 was used for the measurement.

2.3 Reactivity Measurement

SiO_2 (20–30 mesh) was obtained from Qingdao Hailang Silica Gel Drier Factory. Methyl propionate (≥99.0 %) and paraformaldehyde (≥94.0 %), Magnesium nitrate (≥99.0 %) and zirconium nitrate (≥99.0 %), ammonia solution (25 %) and ammonium sulfate (≥99.0 %) are analytical grade.

Titanium(IV) sulfate (≥96.0 %) is chemical grade. Cesium nitrate (99.9 %) is industrial grade.

The reaction was carried out in a fixed-bed reactor at atmospheric pressure. The reactor was made of a stainless steel tube, 42 cm long and 0.8 cm inside diameter, mounted vertically in the furnace. The amount of catalyst was 4 mL and was placed in the middle of reactor. Quartz sands were placed both under and above the catalyst sample. The reaction temperature was in the range of 300–400 °C. The mixed solution of MP, FA and methanol was fed in from the top of the reactor by an advection pump with the feed rate of 0.1 mL/min. The MP/FA/CH_3OH molar ratio was fixed at 1/2/2, unless otherwise indicated. Nitrogen was fed in from the top of the reactor with a fixed feed rate. The contact time was 1.9 s. The samples were collected after 100 min on stream.

In order to reduce the impact of water in the reaction and avoid the hydrolysis of MP and MMA, paraformaldehyde was dissolved in methanol to obtain mixture of formaldehyde and methanol, which was used as a source of HCHO instead of formalin.

The effluent gas from the reactor was led into a condenser and the liquid samples were collected per 45 min interval. After 100 min on run, the reactants and products of gas phase and liquid phase were analyzed by gas chromatography (Agilent 7890A GC). *N*-Heptane was added to the products as an internal standard. The activity of catalyst was measured by testing the conversion of MP; the selectivity and yield of MMA and MAA which were calculated in Eqs. 1–5.

$$\text{Conversion of MP} = \frac{\text{MP}_{\text{in,mol}} - \text{MP}_{\text{out,mol}}}{\text{MP}_{\text{in,mol}}} \times 100 \quad (1)$$

$$\text{Selectivity to MMA} = \frac{\text{MMA}_{\text{out,mol}}}{\text{MP}_{\text{in,mol}} - \text{MP}_{\text{out,mol}}} \times 100 \quad (2)$$

$$\text{Selectivity to MAA} = \frac{\text{MAA}_{\text{out,mol}}}{\text{MP}_{\text{in,mol}} - \text{MP}_{\text{out,mol}}} \times 100 \quad (3)$$

$$\text{Yield of MMA} = \text{Conversion of MP} \times \text{Selectivity of MMA} \quad (4)$$

$$\text{Yield of MAA} = \text{Conversion of MP} \times \text{Selectivity of MAA} \quad (5)$$

3 Results and Discussion

3.1 Catalysts Characterization

3.1.1 XRD Results

Figure 1a presents the XRD patterns of the prepared catalysts with different supports (SiO_2, Al_2O_3, TiO_2 and MgO). The catalysts were prepared with 15 wt% cesium-loading and calcined at 450 °C for 3 h. The cesium nitrate with hexagonal were observed in all catalysts, but few peaks of cesium nitrate were exhibited on the Zr–Mg–Cs/Al_2O_3 catalysts. Figure 1b presented the XRD patterns of Zr–Mg–Cs/SiO_2 catalyst at different calcination temperatures. The cesium nitrate with hexagonal phase was observed in all catalysts, but the intensity of cesium nitrate decreased with increasing calcination temperature. This was attributed to cesium nitrate decomposed and volatilized with increase of the calcination temperature; this phenomenon was also confirmed by TG/DTA analysis.

3.1.2 Thermal Analysis (TG/DTA)

The thermostability of the Zr–Mg–Cs/SiO_2 catalysts was investigated by TG/DTA method. The thermal stability of cesium nitrate was studied and Fig. 2 showed the TG/DTA curves of $CsNO_3$. The first endothermic DTA peak turned up at 158 °C with no weight loss, which attributed to melt of impurities in the cesium nitrate. The second big endothermic DTA peak at 408 °C with no weight loss was due to melting of $CsNO_3$. It was closed to the melting point of $CsNO_3$ which was 414 °C reported in the literature. The weight loss was 97 % between 500 and 800 °C accompanied with the two broad endothermic DTA peak, which was attributed to decomposition and volatilization of $CsNO_3$. For the sample of Zr–Mg–Cs/SiO_2 calcined at 450 °C (Fig. 3a), the weight

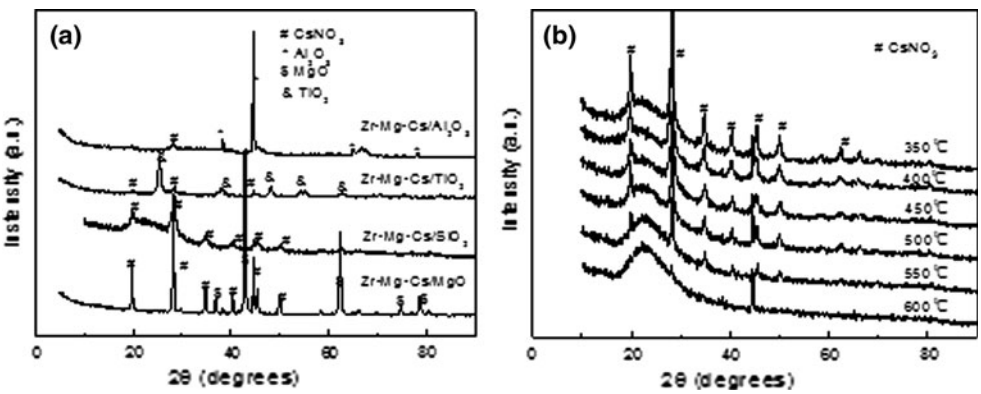

Fig. 1 XRD patterns of the catalysts with different supports (**a**) and calcined at different temperatures (**b**): (*hash*) $CsNO_3$, hexagonal, (*asterisk*) Al_2O_3, rhombohedral (*dollar*) MgO, cubic, (*ampersand*) TiO_2, tetragonal

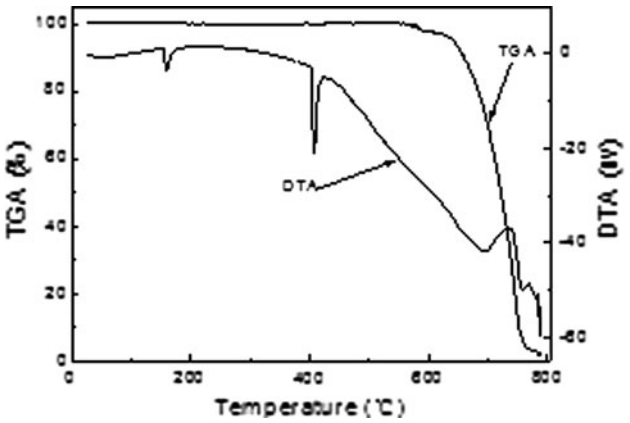

Fig. 2 TG/DTA curves of $CsNO_3$

loss was 1.5 % between 50 and 150 °C with a small endothermic DTA peak at 55 °C, which was attributed to the loss of physical adsorbed water molecules. The second weight loss was 5 % between 500 and 650 °C accompanied a broad endothermic DTA peak at 550 °C, which was attributed to decomposition and volatilization of $CsNO_3$ in the Zr–Mg–Cs/SiO_2 catalyst. For the sample of Zr–Mg–Cs/SiO_2 calcined at 600 °C (Fig. 3b), there was no visible weight loss between 500 °C and 800 °C, this indicates the Zr–Mg–Cs/SiO_2 catalyst calcined at 600 °C, the $CsNO_3$ had completely decomposed. Thus the thermogravimetry studies revealed that the Zr–Mg–Cs/SiO_2 catalyst should be prepared and used below 500 °C.

3.1.3 BET Specific Surface Area Analysis

The physical properties (BET specific surface area, pore volume and mean pore diameter) of the catalysts were presented in Tables 1, 2 and 3, respectively. Table 1 showed the commercial SiO_2 and γ-Al_2O_3 had large specific surface area, while the specific surface area of prepared TiO_2 and MgO were relatively small. The specific surface area of Zr–Mg–Cs/SiO_2 decreased with increasing the calcination temperature, while the mean pore diameter gradually increased (see Table 2). The specific surface area slightly decreased below 500 °C, but the specific surface area sharply declined over 500 °C. This phenomenon may be due to the destruction of pores of SiO_2 at higher temperature. In Table 3, the specific surface area of the catalysts decreased with increasing the content of cesium nitrate. It indicated that cesium nitrate loaded in SiO_2 occupies some channels.

3.1.4 Acidity and Basicity Analysis

The quantitative analysis of base and acid sites on the surfaces of catalysts were determined by stepwise temperature-programmed desorption (TPD) of CO_2 and NH_3. The peaks showed in each of the profiles correspond to desorption of CO_2 and NH_3 related to the base and acid sites of the catalysts surface. The desorption temperature indicates the base and acid strength of the catalysts. The higher temperature of desorption, the stronger base and acid strength of the catalysts [19, 20].

The characteristic CO_2 and NH_3 TPD patterns for each of the four catalysts in Table 1 had been compared in Fig. 4. Figure 4a gave the CO_2 TPD patterns (measuring basicity). The four catalysts had a distinct CO_2 desorption peak between 50 and 250 °C which corresponded to the weak strength base sites. The number density of base sites was greater on the γ-Al_2O_3 and TiO_2 samples than on the SiO_2 sample. Figure 4b showed the acidity of catalysts by NH_3 TPD patterns. The TiO_2 sample presented a desorption peak at 130 °C; the SiO_2 and Al_2O_3 samples presented desorption peaks at 150 °C; and the desorption peak of MgO sample was at 220 °C; which all corresponded to the weak strength acid sites, however, the MgO sample showed a little stronger acidity than the other ones. This may be due to the following reasons. The MgO carrier had minimum specific surface area (14.7 m^2/g); which could be coated by cesium nitrate, so the base sites of MgO were completely covered by cesium nitrate. Cesium nitrate presented a weak acidic substance. Therefore, the acidity of the Zr–Mg–Cs/MgO sample corresponded to the acid sites of cesium nitrate. The γ-Al_2O_3 sample presented another NH_3 desorption peaks (300–500 °C), which corresponded the middle strength acid sites. The acid sites density on the TiO_2 sample was greater than the other samples.

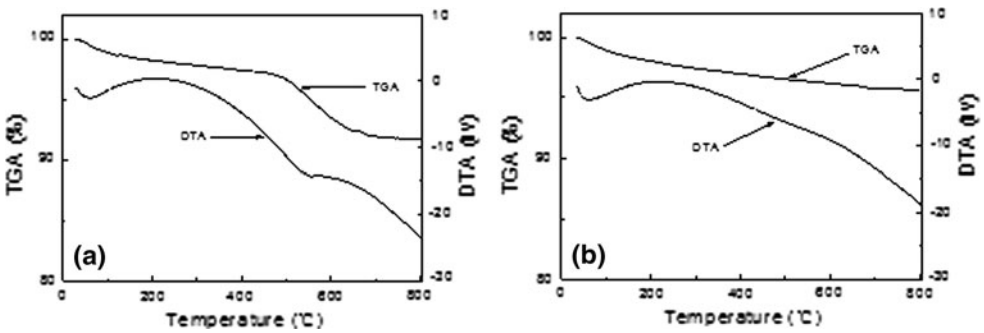

Fig. 3 TG/DTA curves of the Zr–Mg–Cs/SiO_2 calcined at: **a** 450 °C; **b** 600 °C

Table 1 Textural and acid–base property of the catalysts with different supports

Catalysts	S_{BET} (m^2/g)	Pore volume (cc/g)	Mean pore diameter (nm)	Total base amount (μmol/g)	Total acid amount (μmol/g)
Zr–Mg–Cs/SiO_2	275.3	0.706	10.3	4.63	0.43
Zr–Mg–Cs/γ-Al_2O_3	233.4	0.537	9.2	33.09	0.48
Zr–Mg–Cs/TiO_2	58.6	0.126	8.6	18.45	0.67
Zr–Mg–Cs/MgO	14.7	0.349	95.0	5.28	0.30

Cs content was determined by the X-ray fluorescence (PANalytical Axios)

Table 2 Textural and acid–base property of the Zr–Mg–Cs/SiO_2 catalysts calcined at different temperatures

Calcination temperature (°C)	S_{BET} (m^2/g)	Pore volume (cc/g)	Mean pore diameter (nm)	Total base amount (μmol/g)	Total acid amount (μmol/g)
350	291.3	0.724	9.9	5.39	0.28
400	294.4	0.723	9.8	4.71	0.35
450	275.3	0.706	10.3	4.63	0.43
500	254.4	0.724	11.4	4.34	0.50
550	114.2	0.641	22.5	3.70	0.66
600	76.5	0.642	33.6	3.02	0.87

Table 3 Textural and acid–base property of the Zr–Mg–Cs/SiO_2 catalysts loaded with different amount of cesium

Amount of cesium (wt%)	S_{BET} (m^2/g)	Pore volume (cc/g)	Mean pore diameter (nm)	Total base amount (μmol/g)	Total acid amount (μmol/g)
0	414.3	0.958	9.2	1.09	0.99
3	363.5	0.872	9.6	1.78	0.27
5	345.3	0.866	10.0	3.02	0.31
10	292.6	0.763	10.4	4.26	0.36
15	275.3	0.706	10.3	4.63	0.43
20	230.3	0.596	10.4	5.27	0.46

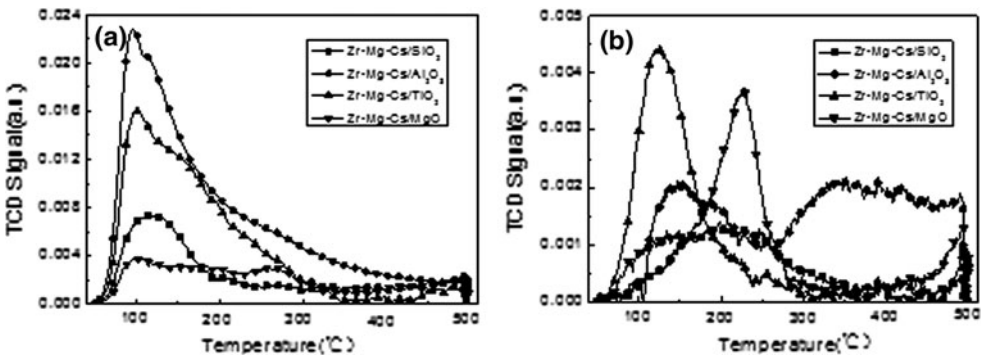

Fig. 4 TPD curves of the catalysts with different supports in atmosphere of: **a** CO_2; **b** NH_3

The characteristic CO_2 and NH_3 TPD patterns for Zr–Mg–Cs/SiO_2 catalysts at different calcination temperature were compared in Fig. 5. Figure 5a showed the desorption profiles of CO_2 from Zr–Mg–Cs/SiO_2 catalysts. All catalysts exhibited a prominent CO_2 desorption peak in the range of 50–250 °C, the basic sites on these catalysts were considered to be weak. Increasing calcination temperature of catalyst decreased the CO_2 adsorption capacity, indicating some base sites were disappeared on the catalyst surface. Figure 5b showed the desorption profiles of NH_3 from Zr–Mg–Cs/SiO_2 catalysts. The NH_3 adsorption capacity increased with increasing calcination temperature.

Figure 6 compared the desorption profiles of CO_2 and NH_3 from SiO_2 supported different loadings of cesium catalysts. Figure 5a gave the CO_2 TPD patterns. Adding more cesium to the SiO_2 increasing its CO_2 adsorption capacity significantly, indicating new base sites were formed on the surface. Figure 5b gave the NH_3 TPD patterns. Adding cesium only slightly affect the NH_3 adsorption capacity. The total amount of acid and base sites on the

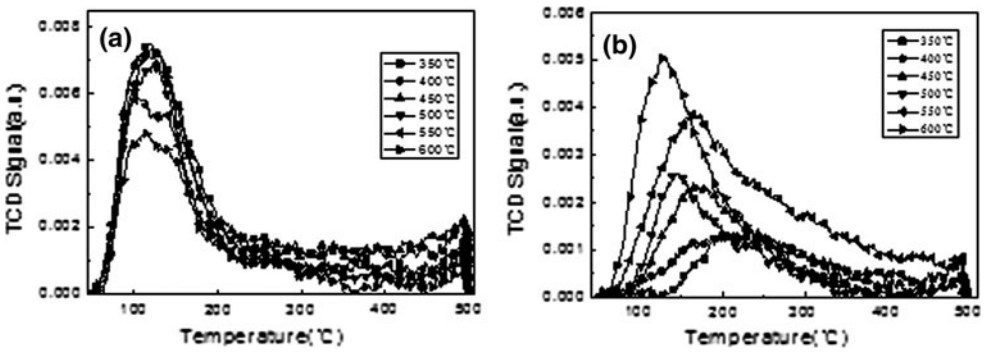

Fig. 5 TPD curves of the Zr–Mg–Cs/SiO_2 catalyst calcined at different temperatures in atmosphere of: **a** CO_2; **b** NH_3

catalysts surface were summarized in Tables 1, 2 and 3, respectively. From the view of acid–base analysis, the presence of the low-temperature peak in the range of 50–250 °C directly related to the MMA yield, the amount of base and acid sites directly corresponded to the MP conversion.

3.2 Aldol Condensation of MP with FA

3.2.1 Effects of the Supports

The effects of the supports on the catalytic activity were summarized in Table 4. The catalysts were prepared with 15 wt% cesium-loading and reaction was performed at 360 °C. The samples were collected after 100 min on stream. In this paper, 15 wt% cesium-loading were based on the quality of the carriers. In fact, the theoretical content of cesium was 12.3 % in the entire catalyst. The actual cesium-loading in different carriers were measured by XRF and the results were presented in Table 5. The actual amounts of Cs contained in the SiO_2 and MgO samples were 11.5 and 12.1 %, respectively. These were closed to the theoretical content of cesium (12.3 %).

The Zr–Mg–Cs/SiO_2 catalyst exhibited the best activity for the reaction, and the Zr–Mg–Cs/Al_2O_3 catalyst showed moderate activity. Although the Zr–Mg–Cs/TiO_2 catalyst was active for the conversion of MP, its selectivity to MMA was very poor. The Zr–Mg–Cs/MgO catalyst exhibited little activity for the reaction. In order to maintain constant of residence time, the volume of catalyst should be uniform, so 4 mL of catalysts were used for all reaction. However, due to differences in density of the carriers, the qualities of 4 mL catalysts with different carriers were diverse. Their quality and cesium-loading were summarized in Table 5. For the sake of comparing catalytic activity of active component (Cs) in different carriers, the conversion of MP was also calculated by the unit mass active component (Cs) of the catalyst and the results were showed in Table 5. The conversion of MP on per gram cesium was 0.084 mol/h in the SiO_2 catalyst, which was higher than the other ones. It was indicated that the Zr–Mg–Cs/SiO_2 catalyst had the best catalytic activity. From the results of BET, the SiO_2 and Al_2O_3 samples had large specific surface area and mesoporous about 10 nm; while the specific surface area of TiO_2 and MgO samples was relatively small. It indicated the large specific surface area corresponded to the high yield. From the acid/base analysis, these four catalysts had almost the same strength of base sites, but the strength of acid sites was significantly different. Compared with the Zr–Mg–Cs/SiO_2 sample, the acid strength of Zr–Mg–Cs/TiO_2 sample was weak, while the acid strength of Zr–Mg–Cs/MgO sample was stronger. The mechanism of condensation clearly implied that acidic and basic properties were both needed for a moderate catalyst; and the condensation reaction may be facilitated by a combination of a Brønsted acid site and a base site on the catalyst surface [2]. Our results suggested there may be a possible correlation between the acid–base site

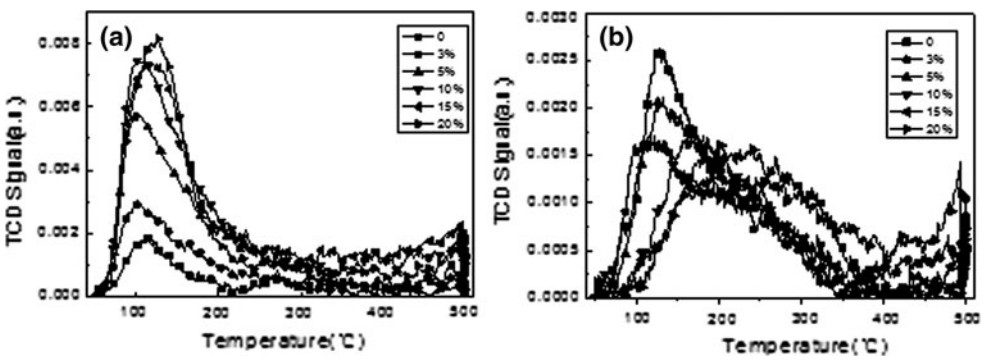

Fig. 6 TPD curves of the Zr–Mg–Cs/SiO_2 catalysts with different amount of cesium in atmosphere of: **a** CO_2; **b** NH_3

Table 4 Effect of the supports on the aldol condensation of MP with FA

Catalysts	X_{MP} (%)	S_{MMA} (%)	S_{MAA} (%)	Y_{MMA} (%)	Y_{MAA} (%)
Zr–Mg–Cs/SiO_2	55.4	75.3	1.3	41.7	0.7
Zr–Mg–Cs/γ-Al_2O_3	34.4	62.2	0.6	21.4	0.2
Zr–Mg–Cs/MgO	16.5	10.2	2.3	1.7	0.4
Zr–Mg–Cs/TiO_2	56.9	13.5	1.5	7.7	0.8

Reaction was performed at 360 °C, Molar ratio of MP/HCHO was ½, feed rate of 0.1 mL/min

X conversion, *S* selectivity, *Y* yield

distribution and the condensation yield, the acid sites at description temperature of 50–300 °C was desired for the selectivity to MMA. In the cases of TiO_2 and MgO catalysts, large amounts of MP were consumed without forming MMA. So we used silica as support to conduct the research on the aldol condensation of MP with FA.

3.2.2 *Effects of Calcination Temperature*

Calcination temperature was an important factor in preparing catalysts since it significantly affected the structure and catalytic properties of catalysts. The Zr–Mg–Cs/SiO_2 catalysts with 15 wt% cesium-loading were calcined at 350, 400, 450, 500, 550 and 600 °C for 3 h, respectively. The reaction was performed at 360 °C.

The effect of calcination temperature on catalytic activity was showed in Fig. 7. The conversion of MP changed slightly at the calcination temperature below 500 °C and was around 55 %, but more than 500 °C, the conversion of MP decreased rapidly. The selectivity of MMA was not affected by the calcination temperature and was around 73 %. From the textural analysis, the specific surface area decreased slightly on the catalysts at the calcination temperature below 500 °C, while it decreased sharply over 500 °C. From the view of TG/DTA, acidity and basicity analysis, cesium nitrate will decompose when the calcination temperature was over 500 °C, and the total amount of base sites on the catalysts surface decreased when increasing the calcination temperature. The decline of surface area and the total amount of base sites with increasing of the calcination temperature might be main

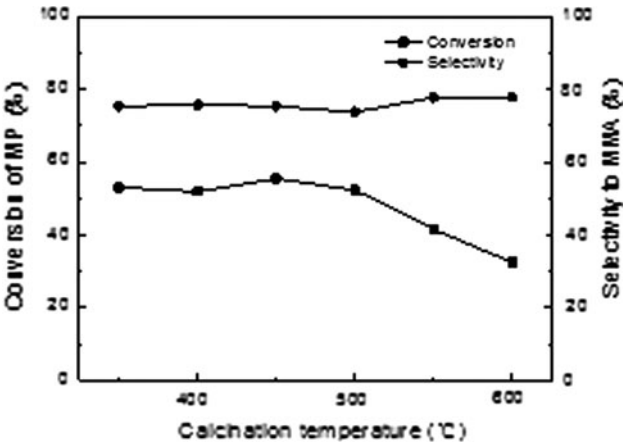

Fig. 7 Effects of calcination temperature on the catalytic performance. Reaction was performed at 360 °C; molar ratio of MP/HCHO was 1/2; feed rate of 0.1 mL/min

factor for the decrease of catalytic activity on the conversion of MP.

3.2.3 *Effects of the Amount of Cesium Supported on Silica*

The reaction was performed on the Zr–Mg–Cs/SiO_2 catalysts with six different cesium loading, namely, 0, 3, 5, 10, 15 and 20 wt%. All catalysts were calcined at 450 °C. The catalytic activity of the silica catalysts with different amounts of cesium were showed in Fig. 8. The conversion of MP increased rapidly with increasing the loading of the cesium when the cesium loading was below 15 wt%. It appeared to reach a plateau at 15 wt% loading. The conversion of MP increasing slightly when the cesium loading from 15 wt% up to 20 wt%. However, Bailey et al. [21] reported that the catalytic activity for aldol condensation of PA with FA went through a maximum at a cesium loading about 5 % by weight. Tai and Davis [2] also observed that the conversion of PA over the Cs-loaded silica catalysts appeared to reach a plateau at 4 wt% loading for the aldol condensation of PA with FA. This difference in loading of cesium was attributed to the following reasons. First, the silica which we used had a larger surface area than those of Bailey and Tai. Second, it was believed that the aldol condensation reaction with MP was more difficult than that with PA. From the textural, acidity and basicity analysis,

Table 5 Property of the catalysts with different carriers

Catalyst	Cs content (%)	Weight of 4 mL catalyst (g)	Cs content in 4 mL catalyst (g)	Conversion (mol_{MP}/gCs h)
Zr–Mg–Cs/SiO_2	11.5	2.1	0.24	0.084
Zr–Mg–Cs/Al_2O_3	9.8	2.7	0.26	0.048
Zr–Mg–Cs/TiO_2	13.5	4.2	0.57	0.034
Zr–Mg–Cs/MgO	12.1	3.4	0.41	0.015

Cs content was determined by the X-ray fluorescence (PANalytical Axios)

the amount of acid/base sites increased with the increasing of cesium. It provided more active sites for the reaction. These may be the main reason of high conversion for catalysts with high cesium content. The specific surface area decreased with increasing cesium loading, while the catalytic activity gradually strengthened. It indicated the specific surface area was not a key factor for the reaction in our experimental condition.

3.2.4 *Effects of Reaction Temperature*

The reaction was performed on the Zr–Mg–Cs/SiO_2 catalyst which was calcined at 450 °C with 15 wt% cesium. The molar ratio of MP/FA/CH_3OH was 1/1/1.5; the reaction temperature range from 300 to 400 °C. The result was showed in Fig. 9. The conversion of MP increased with increasing of the reaction temperature, while the selectivity proceeded with the opposite trend. This was attributed to that the more by-products were produced at the higher reaction temperature, so the selectivity of MMA decreased. The maximum yield of MMA was 32.9 % at 380 °C and the selectivity of MMA was 70.3 %.

3.2.5 *Effects of the MP/HCHO Molar Ratio*

The reaction was performed at 360 °C at Zr–Mg–Cs/SiO_2 catalysts with 15 wt% cesium. The effect of the MP/HCHO molar ratio on the reaction was summarized in Table 6. With the increasing of the MP/HCHO molar ratio, the conversion of MP increased from 36.2 to 55.4 %. When the MP/HCHO molar ratio was 1/1, the selectivity to MMA was the best and achieved to 80.3 %.

3.3 Catalyst Stability and Reusability

The stability and reusability of Zr–Mg–Cs/SiO_2 catalyst (cesium loading: 15 wt% and calcined: 450 °C) was also investigated. The reaction was performed at 320 °C; the molar ratio of MP/FA was 1/1. Figure 11a showed the yield of MMA based on the MP feed as function of the time-on stream. The activity dropped by nearly 50 % after reacting of 32 h. The deactivation mechanism may be due to the formation of carbonaceous deposits on the surface of the catalyst. In fact, the catalyst turned black after use [22, 23]. The carbon content of the fresh and used catalysts was

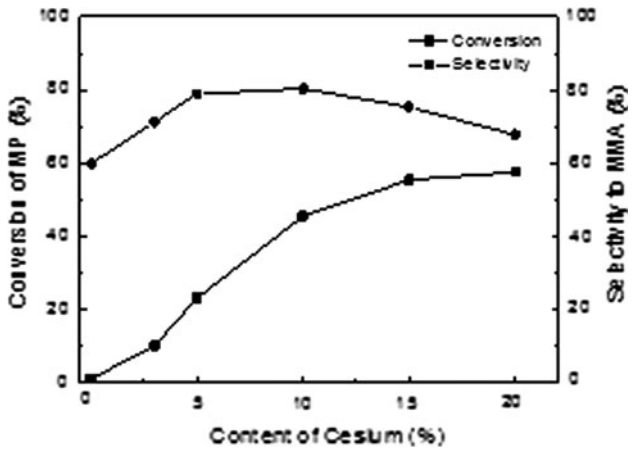

Fig. 8 Effects of the amount of cesium on the catalytic performance. Reaction was performed at 360 °C; molar ratio of MP/HCHO was 1/2; feed rate of 0.1 mL/min

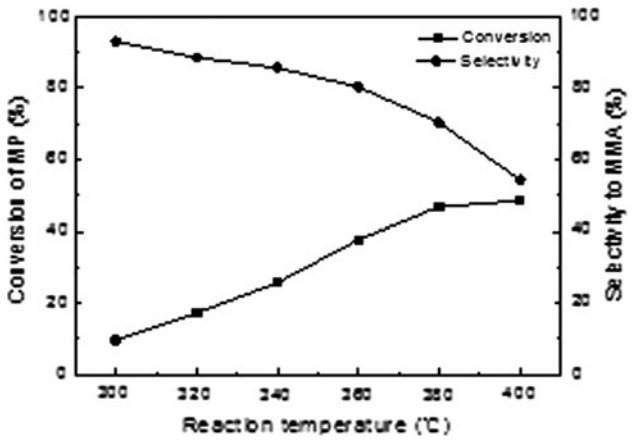

Fig. 9 Effects of reaction temperature on the catalytic performance. molar ratio of MP/HCHO was 1/1; feed rate of 0.1 mL/min

Table 6 Effect of the MP/HCHO molar ratio on the aldol condensation of MP with FA

Molar ratio of MP/HCHO	X_{MP} (%)	S_{MMA} (%)	S_{MAA} (%)	Y_{MMA} (%)	Y_{MAA} (%)
1/0.5	36.2	73.7	0.7	26.5	0.2
1/1	37.7	80.3	2.1	30.2	0.8
1/2	55.4	75.3	1.3	41.7	0.7

Reaction was performed at 360 °C, feed rate of 0.1 mL/min

X conversion, *S* selectivity, *Y* yield

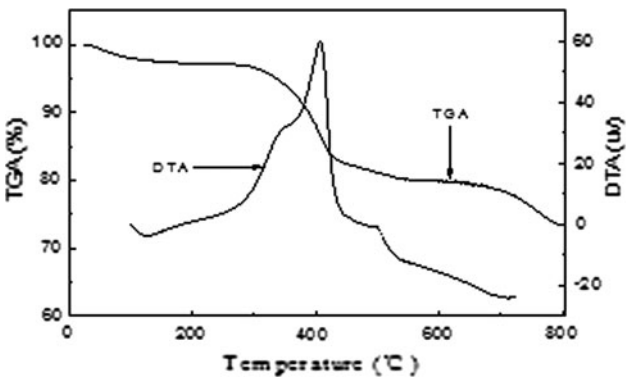

Fig. 10 TG/DTA curves of the used Zr–Mg–Cs/SiO_2 catalyst after reaction

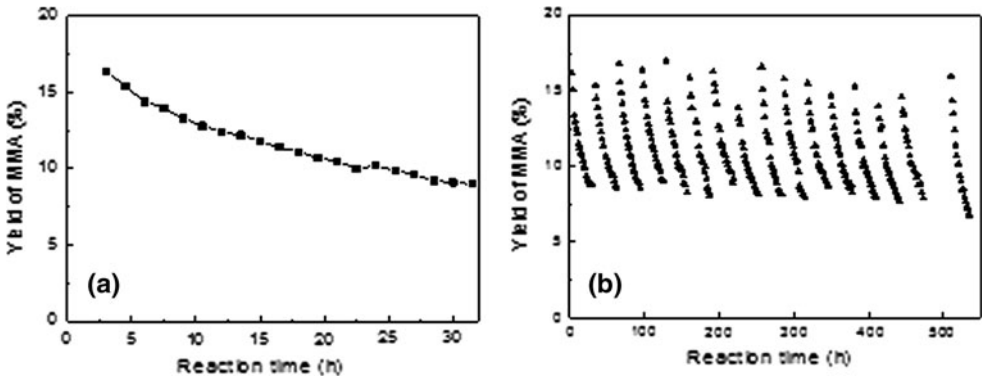

Fig. 11 Yield of MMA on the fresh (**a**) and regenerated catalyst (**b**). Reaction was performed at 320 °C; molar ratio of MP/HCHO was 1/1; feed rate of 0.1 mL/min

Table 7 Element content of the fresh and regenerated catalyst

Catalyst	Cesium (%)	Magnesium (%)	Zirconium (%)
Fresh catalyst	11.73	0.046	0.036
Regenerated catalyst	11.31	0.065	0.040

Regenerated catalyst: The 16th regeneration of catalyst

measured by carbon/sulfur analyzer (CS-344, US LECO Corporation). The carbon content of the fresh catalyst was 0.07787 %, while the carbon content of the used catalyst was 3.8461 %. The used catalyst was characterized by TG/DTA (Fig. 10), different from the fresh catalyst, the used catalyst had a distinct weight loss from 300 to 450 °C accompanied with a big exothermic DTA peak at 405 °C, which mainly ascribed to the coke combustion with O_2.

In order to investigate the reusability of the catalyst, the used catalyst was regenerated by calcination in a stream of mixture of oxygen and nitrogen at 450 °C for 3 h, the volume of oxygen was 1 %. The regenerated catalyst was investigated according to the same conditions with the fresh catalyst by reaction 32 h. The catalyst was repeatedly regenerated 16 times and total operation time was over 500 h. Figure 11b showed the catalytic activity of the repeatedly regenerated catalyst. The catalytic properties can be completely restored after regeneration. From the ICP analysis, the content of cesium, magnesium and zirconium in the fresh catalyst and regenerated catalyst (after the 16th regenerated) was showed in Table 7. It indicated that the components of regenerated catalyst did not lose over 500 h. So after the sixteenth regeneration, its activity was still the same as that of the fresh catalyst, which demonstrated that the Zr–Mg–Cs/SiO_2 catalyst had good reusability.

4 Conclusions

The gas aldol condensation reaction of MP with FA to produce MMA was investigated over various catalysts. The cesium-impregnated TiO_2 and MgO carriers presented little activity for the reaction. The conversion and selectivity over the Zr–Mg–Cs/Al_2O_3 catalyst were relatively low. The cesium-impregnated SiO_2 exhibited better catalytic activity and high selectivity for the reaction. The characterization results suggested that the calcination temperature and content of cesium were main factors to affect the textural properties, surface acidity and basicity and catalytic activity of the catalysts. Although the single life of this catalyst was slight short due to carbon deposition on the surface of catalyst, its catalytic activity was completely regenerated by a simple calcination. The Zr–Mg–Cs/SiO_2 catalyst which had good reusability and long cycle life was easily to prepare. Therefore, the Zr–Mg–Cs/SiO_2 catalyst was a promising catalyst for the aldol condensation of MP with FA to produce MMA.

Acknowledgments This work was financially supported by the National natural Science Foundation of China (No. 21076221) and (No. 21276267); National Research Program of China (863 Program) (No. 2012AA062903).

References

1. Nagai K (2001) Appl Catal A 221:367
2. Tai J, Davis RJ (2007) Catal Today 123:42
3. Haeberle T, Emig G (1988) Chem Eng Technol 11:392
4. Ai M (1989) Appl Catal 54:29
5. Lee KY, Oishi S, Igarashi H, Misono M (1997) Catal Today 33:183
6. Shreiber EH, Mullen JR, Gogate MR, Spivey JJ, Roberts GW (1996) Ind Eng Chem Res 35:2444
7. Ai M (2006) Catal Today 111:398
8. Spivey JJ, Gogate MR, Zoeller JR, Colberg RD (1997) Ind Eng Chem Res 36:4600
9. Fouqued G, Merger F, Platz R, Baer K (1978) US Patent 4 118 588
10. Giancarlo A, Pietro M (1983) Appl Catal 6:293
11. Ai M (1988) Appl Catal 36:221
12. Calvino V, Martin R, Sobczak I, Ziolek M (2006) Appl Catal A 303:121
13. Jackson SD, Johnson DW, Kelly JD, Williams BP (2003) US Patent 6 544 924

14. Ai M, Fujihashi H, Hosoi S, Yoshida A (2003) Appl Catal A 252:185
15. Yoo JS (1993) Appl Catal A 102:215
16. Wierzchowski PT, Zatorski LW (1991) Catal Lett 9:411
17. Gogate MR, Spivey JJ, Zoeller JR (1997) Catal Today 36:243
18. Ai M (2005) Appl Catal A 288:211
19. Emil D, Vasile H, Carmen C, Cezar C, Didier T, Robert D (1999) Appl Catal A 178:145
20. Chen H, Xue M, Hu S, Shen J (2012) Chem Eng J 181:677
21. Bailey OH, Montag RA, Yoo JS (1992) Appl Catal A 88:163
22. Ding S, Wang L, Yan R, Zhang S (2012) Adv Mater Res 396:719
23. Mao D, Lu G, Chen Q (2005) J Mol Catal A Chem 240:164